Received: 3 July 2020 | Revised: 4 October 2020 | Accepted: 4 November 2020

DOI: 10.1111/cas.14728

ORIGINAL ARTICLE

Cancer Science WILEY

Intracellular localization of CK2α as a prognostic factor in invasive breast carcinomas

Miwako Kato Homma[1] | Yuichiro Kiko[2] | Yuko Hashimoto[2] | Miki Nagatsuka[3] | Naoto Katagata[3] | Seiichiro Masui[4] | Yoshimi Homma[1] | Tadashi Nomizu[3]

[1]Department of Biomolecular Sciences, Fukushima Medical University School of Medicine, Fukushima, Japan

[2]Department of Diagnostic Pathology, Fukushima Medical University School of Medicine, Fukushima, Japan

[3]Department of Surgery, Hoshi General Hospital, Fukushima, Japan

[4]Medical Research Center, Fukushima Medical University School of Medicine, Fukushima, Japan

Correspondence
Miwako Kato Homma, Department of Biomolecular Sciences, Fukushima Medical University School of Medicine, 1-Hikarigaoka Fukushima 960-1295 Japan.
Email: mkhomma@fmu.ac.jp

Funding information
Japan Agency for Medical Research and Development, Grant/Award Number: 20lm0203006j0004

Abstract

Overexpression of the ubiquitous protein kinase, CK2α, has been reported in various human cancers. Here, we demonstrate that nuclear and nucleolar CK2α localization in invasive ductal carcinomas of the breast is a reliable predictor of poor prognosis. Cellular localization of CK2α in nuclei and nucleoli was analyzed immunohistochemically using surgical tissue blocks from 112 patients, who had undergone surgery without neoadjuvant chemotherapy. Clinical data collection and median follow-up period were for more than 5 y. In total, 93.8% of patients demonstrated elevated CK2α expression in nuclei and 36.6% of them displayed elevated expression predominantly in nucleoli. Clinicopathological malignancy was strongly correlated with elevated nuclear and nucleolar CK2α expression. Recurrence-free survival was significantly worse ($P = .0002$) in patients with positive nucleolar CK2α staining. The 5-y survival rate decreased to a roughly 50% in nucleolar CK2α-positive patients of triple-negative ($P = .0069$) and p Stage 3 ($P = .0073$) groups. In contrast, no patients relapsed or died in the triple-negative group who exhibited a lack of nucleolar CK2α staining. Evaluation of nucleolar CK2α staining showed a high secondary index with a hazard ratio of 6.629 ($P = .001$), following lymph node metastasis with a hazard ratio of 14.30 ($P = .0008$). Multivariate analysis demonstrated that nucleolar CK2α is an independent factor for recurrence-free survival. Therefore, we propose that histochemical evaluation of nucleolar CK2α-positive staining may be a new and robust prognostic indicator for patients who need further treatment. Functional consequences of nucleolar CK2 dysfunction may be a starting point to facilitate development of novel treatments for invasive breast carcinoma.

KEYWORDS

breast cancer, invasive ductal carcinoma, nucleus, prognostic factor, protein kinase CK2

Abbreviations: CI, confidence interval; DSS, disease-specific survival; ER, estrogen receptor; HER2, human epidermal growth factor receptor type 2; HR, hazard ratio; IDC, invasive ductal carcinoma; p N0-p N3, nodal metastatic lymph statue according to UICC classification; p Stage, pathological stage; PR, progesterone receptor; RFS, recurrence-free survival; TN, triple negative.

1 | INTRODUCTION

Breast cancer is the leading type of cancer in women, with *c*. 2.1 million cases in 2018, accounting for 24% of all women with cancer, and the leading cause of death in women with cancer deaths worldwide.[1,2] Although the 5-y survival rate of these patients is relatively high, undesirable recurrences and fatalities do occur. Prognostic information is derived from clinicopathological classification based on tumor size, nodal status, histological grade, and tumor subtype. Immunohistochemical (IH) analysis, combined with expression level assessment of ER, PR, and human epidermal growth factor receptors 2 (HER2), is currently used for subtyping breast cancers, based on the UICC-standardized method.[3] Luminal early breast cancers, which are hormone-sensitive and tend to respond well to hormonal drug treatment, present relatively low recurrence rates following surgery.[4] Breast cancers that are HER2-positive also respond well to anti-HER2 drugs, such as trastuzumab. In contrast, another subtype, classified as triple negative, recurs at higher rates with metastases, in spite of aggressive treatment with chemotherapy and/or radiotherapy. There are several valuable indicators of cancer relapse, such as lymph node status or Ki-67 labeling index, however these cannot predict distant recurrence in hormone receptor-negative or even in hormone receptor-positive patients who showed no lymph node metastasis, or who had been diagnosed at an early stage after the first surgery. In the United States and Europe, the 21-Gene Recurrence Score Assay and other genomic signatures have been introduced for standardized relapse risk assessment in hormone receptor-positive and HER2-negative breast cancer in its early stages.[5] These genomic signature assays are recommended for guiding adjuvant treatment decisions in patients with hormone receptor-positive breast cancer, for whom the benefit of chemotherapy is unclear. The St. Gallen Consensus panel also concluded that patients with both hormone receptor- and HER2-positive subtypes, together with a high Ki-67 labeling index, should be considered for adjuvant chemotherapy, including those with high recurrence scores of a gene signature assay or histological grade 3.[6] Nonetheless, problems still remain. The optimal Ki-67 cut-point is unclear, and the gene signatures assays are not available for all patients who need them, because they are so costly, even in the USA, Europe, and Japan. Therefore, there is a need to thoroughly understand cancer pathology and to develop the most appropriate strategy combined with reliable prognostic indicators for treatment of all patients.

CK2 is a serine/threonine kinase that is indispensable for eukaryote development and survival. The first observation linking CK2 with malignancy was reported in CK2α, the catalytic subunit of CK2, introduced in transgenic mice, in which 9 of 139 mice developed lymphoma.[7] Increased expression of CK2α transcripts and/or protein has been observed in various types of human cancer[8] and is considered to be one of the driver kinases for oncogenesis,[9] but its functional role needs to be clarified, along with the cancer stem cell pathway.[10] In normal, quiescent, cultured fibroblasts, CK2α presents a predominantly cytoplasmic distribution, however upregulation of nuclear CK2 protein levels has been observed in squamous cell carcinoma of the head and neck[11] and breast carcinoma,[12] both with poor clinical outcomes. Clinical trials using a highly specific and ATP-competitive CK2α inhibitor, CX-4945 for treatment of various cancers, are ongoing in the USA and EU[13] We reported translocation of CK2α from the cytosol to the nucleus during cell cycle progression after growth stimulation of serum-deprived quiescent cells; constituents of nuclear CK2 complexes were involved in RNA processing, chromatin assembly, and ribosomal RNA transcription, which illuminated the participation of this kinase pathway in nuclear functions.[14]

In this study, we further advanced previous findings on cancer-related disorders by evaluating nuclear CK2 complexes in MCF-7 breast cancer cells. The analysis functionally links nuclear CK2 to protein synthesis and to RNA damage and repair. To understand the molecular role of CK2 expression in human cancer, we further employed immunohistochemical staining by examining surgical specimens of IDC of the breast, to evaluate CK2 protein levels and subcellular localization. Our results revealed that CK2 localization in the nucleolus correlates strongly with aggressive tumor behavior and poor clinical outcomes, suggesting "nucleolar positive staining of CK2α" as an independent marker of unfavorable prognoses in IDC. Understanding CK2 function in cancer cell nucleoli may help to improve clinical outcomes.

2 | MATERIALS AND METHODS

2.1 | Patients

Material was derived from 112 patients with stages 1-3 IDC who had undergone surgery at Hoshi General Hospital from 2008 to 2014 without neoadjuvant chemotherapy. Clinicopathological information and outcomes for more than 5 y were confirmed. Stage 4 cases were not included. Clinicopathological parameters were determined according to UICC classification.[3] All were categorized by p Stage after post-operative pathological diagnosis. Follow-up duration was defined as the period between the operation date and day of the last visit, according to the patient's medical record. This retrospective study was approved by the institutional review boards of Fukushima Medical University in August 2018 and Hoshi General Hospital in July 2018. Nodal metastatic status was unknown in 1 case in a patient who was 98 y old, with no lump upon palpation, no metastasis on the image, and negative results upon cytological examination of lymph nodes by ultrasound diagnosis. Therefore, for this patient only, we did not search the axilla during surgery.

2.2 | Immunohistochemistry

Cellular localization of CK2α was analyzed immunohistochemically. Paraffin-embedded surgical tissue blocks were sectioned at 4 μm and transferred to adhesive microscope slides (Platinum Pro: Matsunami Glass Ind., Ltd.). Negative controls lacked only the primary antibody in an identical procedure. After rehydration and

antigen retrieval, samples were autoclaved at 121°C for 10 min in 10 mmol/L citrate-Na buffer at pH 8.0. Antigen blocking was performed using normal serum (Vector Laboratories, Inc) at a dilution of 1:200, and slides incubated for 30 min at room temperature. Slides were subsequently incubated with primary antibody, monoclonal anti-CK2α (code: 70774, Abcam) overnight at 4°C at a dilution of 1:1000 in phosphate-buffered saline containing 1% bovine serum albumin. Detection of immune-reactive staining was performed using the avidin-biotin-peroxidase complex method, in accordance with the manufacturer's instructions (ABC Kit: Vector Laboratories Inc). After incubation with diaminobenzidine (Dojindo) for 40-80 s, slides were mounted for microscopic interpretation along with control specimens, which were mounted on all slides from 112 clinical samples, and coverslipped under DePex. Sections were not counterstained with hematoxylin to avoid false-positive staining of nucleoli. Immunoreactivity was scored independently by 2 pathologists (Y. Kiko and Y. Hashimoto). At least 3 invasive areas, with the average number of cells in the thousands, were randomly selected by pathologists, and the category of CK2 staining of each plate was evaluated. In a very few cases, when there was heterogeneity of CK2 staining, 3-5 invasive regions were selected at random and evaluated by the category with the largest number of cells. The same method was used by multiple pathologists to obtain the same results. In all cases, multiple pathologists made the same decision and achieved the same results. Ki-67 labeling index was evaluated using anti-human Ki-67 monoclonal antibody, MIB-1 (code: IR626, Dako NY), and an Envision Kit (Dako NY) in accordance with the manufacturer's recommendation, following antigen retrieval with Tris-EDTA antigen retrieval buffer (pH 8.0). Clinical data collection and immunoreactivity were performed independently in an investigator-blinded study.

2.3 | Cell culture

Human retinal pigment epithelial (RPE) cells, human cervical cancer HeLa cells, human colorectal adenocarcinoma SW-480, and human breast invasive ductal carcinoma of breast MCF-7 cells, which are ER-positive, PR-positive, and HER2-negative, were obtained from the American Type Culture Collection and maintained in growth phase at 37°C in a 5% CO_2 in air atmosphere in Dulbecco's modified minimal essential medium containing F12 medium (DMEM-F12, Sigma) for RPE, or RPMI (Sigma) for human cancer cells, supplemented with 10% fetal bovine serum in the absence of antibiotics.

2.4 | Cell fractionation and western blotting

Logarithmically growing cells were harvested in phosphate-buffered saline with a rubber scraper, centrifuged, and lysed to separate cytosolic and nuclear fractions, according to a protocol previously described.[14] To facilitate mass spectrometry, no detergent was included in the fractionation process. Briefly, after removal of the cytosolic fraction, nuclear proteins were solubilized with 0.6 mol/L NaCl in 20 mmol/L HEPES (pH 7.4), containing 25 mmol/L β-glycerophosphate, 20% glycerol, 1 mmol/L DTT, 2 mmol/L EDTA, 1 microgram/mL aprotinin, 1 microgram/mL loupe-tin, 1 mmol/L PMSF. Cytosolic and nuclear fractions from RPE, HeLa, SW-480, and MCF-7 cells were separated by 10% SDS-PAGE, followed by western blotting. The mouse anti-β-actin (A2228, Sigma-Aldrich) and rabbit anti-hnRNPM (SAB450, Sigma-Aldrich) were purchased from commercial sources.

2.5 | Proteome analysis

To identify CK2-associated proteins, nuclear fractions were precleared by extensive incubation with normal IgG-agarose beads, and then immunoprecipitated with anti-CK2α monoclonal antibody previously crosslinked to agarose beads in accordance with the manufacturer's protocol. Proteins associated with the beads were eluted stepwise in 5 fractions with 0.1% formic acid. These eluates were monitored for CK2α protein by western blotting and fractions containing CK2α were combined, digested with trypsin, reduced, and alkylated with dithiothreitol and iodoacetamide, respectively, and prepared for mass analysis as described. To characterize CK2-associated proteins systemically, nuclear and nucleolar extracts were prepared[15,16] more than 5 times independently. We decided to use the nuclear extract instead of the nucleolar fraction to compare CK2-associated proteins between RPE and MCF-7, because of the small number of proteins in RPE nucleolar extracts. Peptide solutions were analyzed using a direct nano-flow liquid chromatography system (Thermo Fischer Scientific) connected to a linear ion trap mass spectrometer (LTQ Orbitrap Velos, Thermo Fisher Scientific). Acquisition of MS/MS spectra was performed, and .raw files were converted into complete peak lists using Xcalibur software. They were analyzed with Proteome Discoverer (v.1.4, Thermo Scientific) for database searching. Protein identification was performed with automated database searches using Mascot (v.2.4, Matrix Science) and the Swiss-Prot database. Protein identification was based on peptide thresholds with a 95.0% confidence minimum, peptide cutoff scores greater than 10, PSMs with delta Cn scores better than 10, protein score thresholds (Mascot) greater than 29, and protein significance with a 95.0% confidence minimum. We analyzed each data set from a minimum of 3 independently prepared samples. ANOVA calculations were performed to obtain semi-quantitative estimates of protein changes and to normalize these quantities against 3 similar samples of MCF-7 and RPE cells, according to the top 3 precursor intensities using the Scaffold 4 algorithm.

2.6 | The sources searched

Proteins in MCF-7 cells were further analyzed using the Ingenuity Pathway Analysis system (Qiagen) to demonstrate their intracellular signal pathways and functions in the cells (10 November 2019 to 30 March 2020). On 23 February 2020, we used publicly available

resources NOD, Nucleolar Localization Sequence Detector: http://www.compbio.dundee.ac.uk/www-nod/, to assess corresponding sequence in human CK2.

2.7 | Statistical analysis

Differences in nucleolar CK2α expression in tumors and clinicopathological parameters (tumor size, lymph node metastasis, histological malignancy, Ki-67 labeling index, recurrent state, mortality, the length of RFS and/or DSS) were examined in this study. CK2 staining was evaluated in relation to tumor recurrence and mortality from breast cancer. Furthermore, survival curves for nucleolar CK2 staining-positive (categories IV and V) and nucleolar CK2 staining-negative (categories I-III) were analyzed using the Kaplan-Meier method. Relapse-free survival and DSS were analyzed. RFS and DSS are defined as the time from surgery to relapse, and the time from surgery to death from breast cancer, respectively. Significance of the difference between the 2 survival curves (nucleolar CK2 positive and nucleolar CK2 negative) was assessed using the log-rank test. The HR and its 95% confidence interval were calculated. A P-value < .05 was considered significant. All statistical analyses were performed using JMP Pro v.14.2.0 (SAS), except the Kaplan-Meier method, which was performed using GraphPad Prism v.7.0. Both platforms were used to draw the same conclusion to investigate the effect of any explanatory variable on RFS.

3 | RESULTS

3.1 | Nuclear CK2α complexes for protein synthesis

Given the importance of nuclear CK2 in cell proliferation, we wondered how CK2 contributed to cell proliferation and whether CK2 was also involved in cellular malignancies. To answer these questions, the protein interactome of nuclear CK2α was investigated using the MCF-7 adenocarcinoma cell line, isolated from a metastasis of a patient with breast cancer. Using western blots, we confirmed prominent expression of CK2α in the nuclei of cancer cells (Figure S1A) compared with that in normal retina-derived cells (RPE). Nuclear proteins were further prepared from MCF-7 and RPE cells followed by immunoprecipitation with CK2α antibody. Proteins significantly elevated in MCF-7 cells are listed in Table S1, and categorized into canonical pathways under Gene Ontology terms EIF2, P70S60, and mTOR signaling, all of which drive cellular functions related to protein synthesis (Figure S1B,D). Putative molecular and cellular functions and top networks suggested CK2α's role in protein synthesis, RNA damage and repair, and RNA post-transcriptional modification in the nuclear compartment (Figure S1C,D). One of the top network terms highlighted CK2α's involvement in cancer signaling. These results prompted us to analyze clinical samples from patients with cancer.

3.2 | CK2 localization to cancer cell nuclei

Between September 2007 and February 2014, 112 patients who developed IDC were admitted for surgery at Hoshi General Hospital in Fukushima, Japan (Table 1). All patients were new cases. Patients with recurrent or bilateral breast cancer at the time of surgery were excluded from this study. None of the patients had received chemotherapy or endocrine therapy preoperatively. Luminal-type (71/112, 63.4%), HER2 type (23/112, 20.5%), and TN breast cancers (18/112, 16.1%) were included (Table 1). When anti-CK2α antibody and diaminobenzidine (DAB) staining were employed with formalin block paraffin-embedded surgical specimens, distinctive nuclear CK2α expression was visible in invasive cells as dots of enhanced density in the nuclei, compared with staining observed in non-invasive cells

TABLE 1 Patient characteristics

Total	n = 112
Median age, y (range)	55 (26-98)
Gender (male/female)	0/112
Tumor size, cm (range)	2.47 (0.1-12)
Subtypes, n (%)	
Luminal: Hormone receptor (+), HER2 (−)	71 (63.4)
HER2: Hormone receptor (−), HER2 (+)	23 (20.5)
Triple negative	18 (16.1)
Histology	
Invasive ductal carcinoma	112
Pathological stage, n (%)	
I	45 (40.2)
IIA	34 (30.4)
IIB	12 (10.7)
IIIA	8 (7.1)
IIIB	1 (0.9)
IIIC	12 (10.7)
Lymph node, n (%)	
p N0	62 (55.3)
p N1	31 (27.7)
p N2	6 (5.4)
p N3	12 (10.7)
Unknown	1 (0.9)
Histological grade, n (%)	
1	25 (22.3)
2	53 (47.3)
3	34 (30.4)
Ki-67, % (range)	19.1 (0.2-77.9)
Recurrence, n (%)	12 (10.7)
Mortality, n (%)	5 (4.5)

Note: Clinicopathological characteristics of IDC samples examined in this study are summarized. Patient demographics and sample characteristics by age, tumor size, tumor subtype by hormone receptor and HER2 status, histology, pathological stage, lymph node status, histological grade, and outcomes are presented.

(Figure 1A). To define the subcellular localization of CK2, we focused on invasive regions of every specimen and defined 5 levels of CK2α expression:

I Nuclear staining was not visible, but cell bodies were stained.
II Nuclear staining was more obvious compared with cytosolic staining.
III Nuclear staining was more intense than in category II.
IV Positive nucleolar staining was evident, as well as nuclear staining.
V Staining was mostly confined to nucleoli, but without intense staining of the nucleoplasm (Figure 1B).

CK2α staining was localized to cell nuclei in 105 of 112 IDC samples (93.75%; Table 1b). CK2 staining categories were compared with important clinicopathological states. Higher median values for tumor size, nodal metastatic status, histological grade, and Ki-67 labeling index were associated with more intense CK2α staining categories, with *P*-values varying from 0.1888 to 0.5737 (Figure 2A). No sample with CK2 staining category I corresponded to histological grade 3, and increasing histological grade was correlated with nucleolar CK2 staining. In histological grade 3, the proportion of CK2 staining categories II plus III (nucleolar negative) was 28.1% (18/64) and of categories IV plus V (nucleolar positive) was 36.6% (15/41). These findings prompted us to examine nuclear localization of CK2 in relation to clinical outcomes in breast carcinomas.

3.3 | Nucleolar CK2 is associated with clinical outcomes

We investigated CK2 staining in subcellular compartments in relation to clinical outcomes, breast cancer recurrence rates, and mortality. Of 112 patients, 12 (10.7%) suffered breast cancer recurrence, including 5 fatalities (4.5%) (Table 2). Two additional patients died of factors other than breast cancer progression. All fatalities resulting

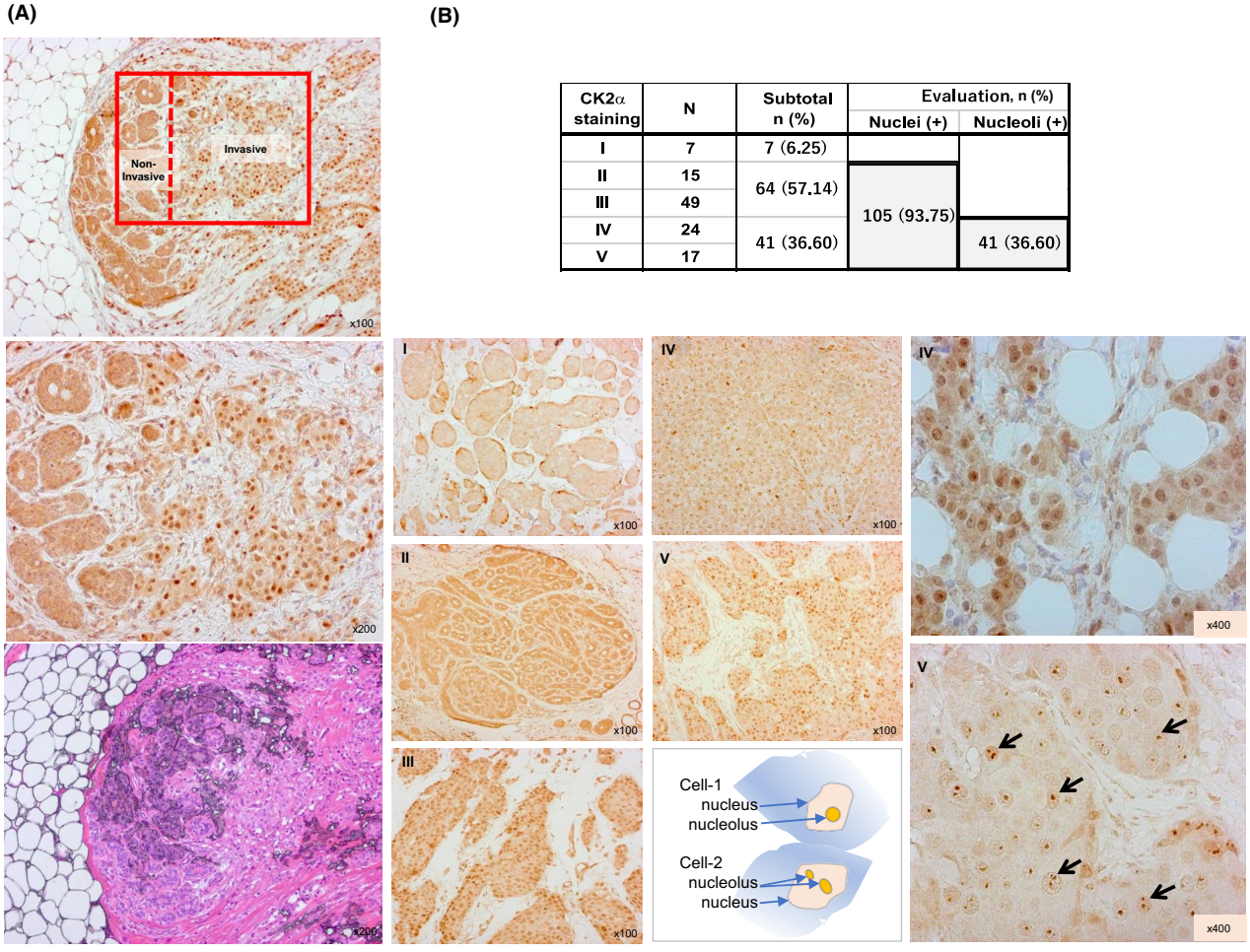

CK2α staining	N	Subtotal n (%)	Evaluation, n (%)	
			Nuclei (+)	Nucleoli (+)
I	7	7 (6.25)		
II	15	64 (57.14)	105 (93.75)	
III	49			
IV	24	41 (36.60)		41 (36.60)
V	17			

FIGURE 1 Detection of nuclear protein kinase CK2α by immunohistochemical analysis of IDC breast carcinomas. A, Representative detection of nuclear protein kinase CK2α in invasive cells. (*Upper*) Paraffin sections were stained with a monoclonal, anti-CK2α antibody, which was detected with diaminobenzidine (DAB). Boxed regions show magnified images and are shown in the *middle* column. (*Lower*) HE staining of a serial section. B, Representative results of CK2 staining categories I, II, III, IV, and V are shown, along with enlarged images for categories IV and V. Arrows indicate positions of nuclei in which nucleolar staining is visible in the center area. (*Upper*) A table represents the distribution of clinical samples and their numbers

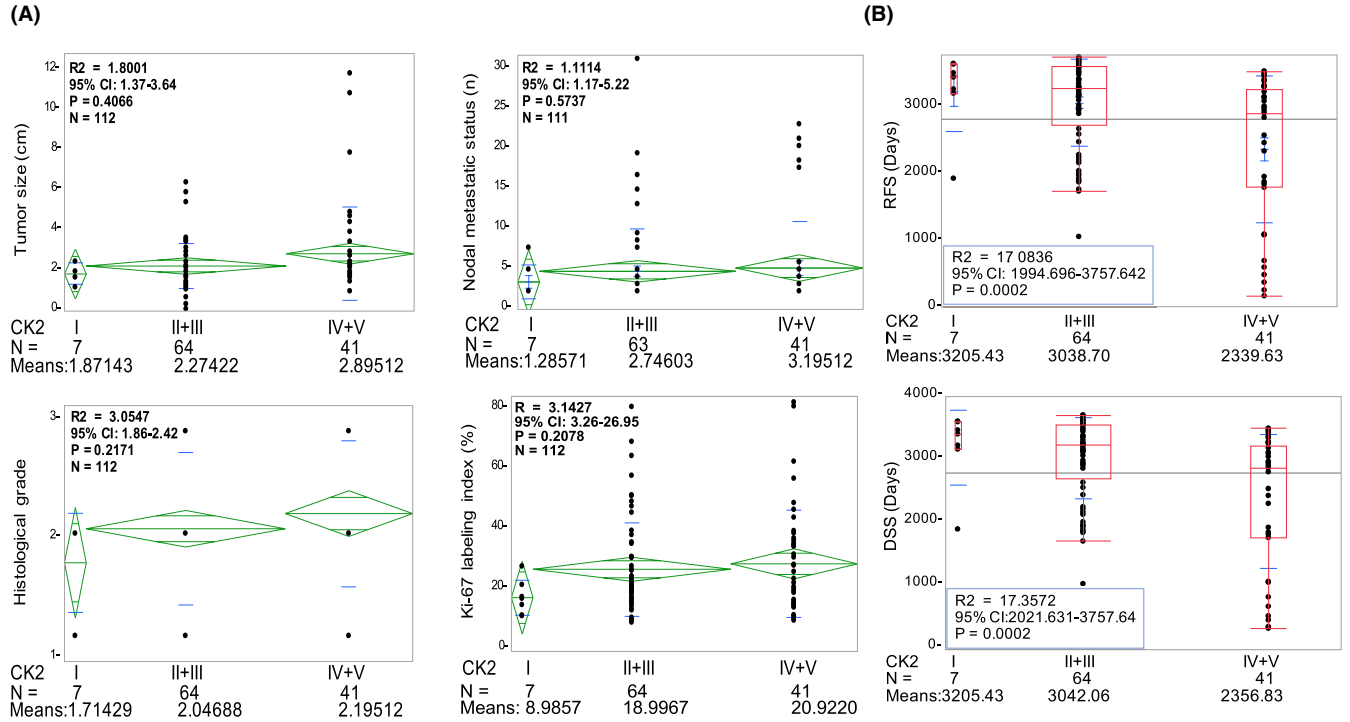

FIGURE 2 Clinical and histological grades are positively correlated with CK2 staining status, which accurately predicts RFS and DSS of breast carcinoma patients. A, Tumor size (*upper left*), metastatic nodal status (*upper right*), histological grade (1-3, *lower left*), and Ki-67 labeling index (%) (*lower right*) are plotted against CK2 staining categories: cytoplasmic CK2 staining only (I), cytoplasmic and nuclear staining (II + III), nuclear and nucleolar staining (IV) plus nucleolar staining (V) samples. B, Box plots showing that patients displaying only cytoplasmic CK2 staining had longer RFS (*upper*) and DSS (*lower*) than patients showing nuclear and nucleolar CK2 staining. Nucleolar CK2-positive staining cases show the shortest RFS and DSS. CI, confidence interval. Means for one-way ANOVA are indicated

TABLE 2 Comparison of patient outcomes and subtype categories between CK2α staining status

		Outcomes related to IDC		Dead	Subtype		
CK2α staining	n (%)	Recurrent	Dead	(total)	Luminal	HER2	TN
I	7 (100)	0	0	0	7 (100)	0	0
II	15 (100)	0	0	0	13 (86.7)	1 (6.7)	1 (6.7)
III	49 (100)	3 (6.1)	1 (2.0)	1 (2.0)	27 (55.1)	11 (22.4)	11 (22.4)
IV	24 (100)	5 (20.8)	2 (8.3)	3 (12.5)	14 (58.3)	8 (33.3)	2 (8.3)
V	17 (100)	4 (23.5)	2 (11.8)	3 (17.6)	10 (58.8)	3 (17.6)	4 (23.5)
Total	112 (100)	12 (10.0)	5 (4.5)	7 (6.3)	71(63.4)	23 (20.5)	18 (16.1)

Note: Summary of survival and fatal recurrences, and subtype categories of breast carcinoma stratified by CK2 staining category, divided into categories of CK2 staining (columns). Luminal: ER and PR, either (+) or both (+), and HER2 (−); HER2: ER (−), PR (−), HER2 (+); TN: ER (−), PR (−), HER2 (−).

from cancer recurrence exhibited CK2 staining levels III, IV, or V. Specifically, nucleolar CK2 staining categories (IV and V) included 41 patients. Nine of these (9/41, 22.0%), suffered cancer recurrence and 4 related to the first breast carcinoma proved fatal (4/41, 9.8%). In contrast, CK2 staining categories I-III comprised 71 patients, only 3 of whom (3/71, 4.2%) suffered a recurrence, with 1 fatality (1/71, 1.4%) (Table 2). Kaplan-Meier analysis demonstrated that RFS and DSS in nucleolus-positive CK2 staining categories (IV + V), were significantly shorter than those associated with categories I-III ($P = .0002$, Figure 2B). These changes were similarly observed in the length of DSS (Figure 2B) and were significant in recurrent and fatal cases (Table S2). These results suggested that nucleolar CK2 localization correlated strongly with poor clinical outcomes.

3.4 | Positive nucleolar CK2 staining predicts poor prognosis

In Kaplan-Meier analysis, we observed a significant difference in cumulative RFS between CK2 staining categories (IV and V) and

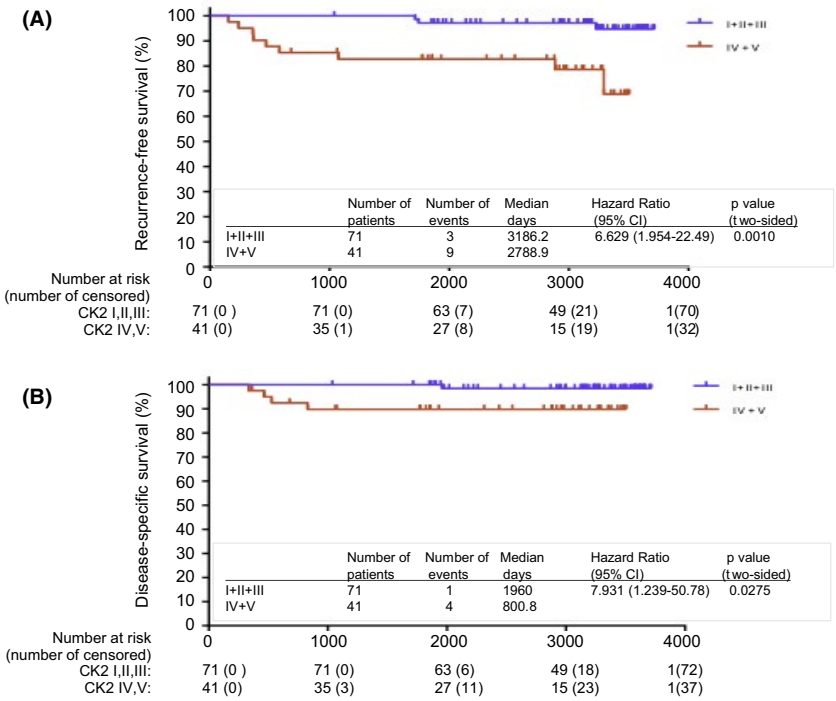

FIGURE 3 Nucleolar CK2α staining is associated with poor outcomes of IDC patients. Percentages of RFS (A) and DSS (B) after the first operation are stratified by nucleolar CK2-positive (IV, V) or – negative (I-III) immunoreactivity using the Kaplan-Meier method. Differences between subcategory curves were assessed using the log-rank test. CI, confidence interval

categories I-III in the 10 y after the first surgery (Figure 3A). DSS analysis presented a similar picture (Figure 3B). When patients were grouped into various clinicopathological subtypes (Figure 4A-E): hormone receptor (ER and/or PR)-positive/HER2-negative, luminal-type breast cancers, which generally responded well to endocrine therapy ($P = .0049$), triple negative ($P = .0069$), p Stage I and p Stage II ($P = .0177$), p Stage III ($P = .0073$), p N I-III ($P = .0138$) or hormone receptor (ER and PR)-negative ($P = .0201$), decreased RFS was also evident in nucleolar CK2-positive cases compared with negative cases. Notably, for the TN group, no patient exhibiting nucleolar CK2-negative staining relapsed or died. In contrast, roughly a 50% decrease of RFS length occurred in nucleolar CK2-positive patients in TN and late-stage groups. Therefore, we suspected that poor RFS and nucleolar CK2 staining are associated with clinicopathological malignancy. We analyzed the HR to assess the prognostic potential of multiple diagnostic factors. As generally recognized, the number of lymph node metastases was the most reliable factor, with the highest HR among them (HR = 14.30, $P = .0008$; Table 3). Evaluation of nucleolar CK2-positive staining showed a high secondary index with HR = 6.629 ($P = .001$), which was significantly higher than the HRs from tumor size or p stage. We further analyzed Cox proportional hazard regression to delineate the effect of any explanatory variable on RFS, in which 2 analytical platforms were used to confirm the same conclusion. Evaluation of nucleolar CK2 can be considered as an independent prognostic factor, as it reached statistical significance in both univariate (HR = 6.853, $P = .004$) and multivariate analyses (HR = 5.264, $P = .017$) (Table 3). In addition, the HR of nucleolar CK2-positive was less affected by adjustments in Cox proportional multivariate analysis, although that of the other 3 factors greatly decreased the ratio. In regard to RFS, we noticed that 3 patients who had fatal outcomes that were diagnosed at p Stage I or IIA at the time of the first operation were accurately evaluated, having nucleolar CK2 staining categories IV or V (Figure S2, Table S2). These results demonstrated the utility of subcellular CK2 distribution as an independent prognostic factor for breast cancer behavior 5-10 y after surgery.

Finally, these conclusions were further strengthened by cluster analysis that grouped patients based upon common attributes and created a decision tree. We used the Partition platform to predict the length of patient RFS, based upon multiple clinicopathological factors presented in a decision tree (Figure S3). The results showed that nucleolar CK2-positive staining (categories IV and V) contributed the most to predicting the variation in future length of survival.

4 | DISCUSSION

Our findings documented the presence of CK2α in cell nucleoli in paraffin-embedded sections of breast cancer tissue from patients who had poor prognoses. Patients with high CK2 expression levels in nucleoli exhibited decreased RFS ($P = .001$) after surgery. There were no fatalities among patients in CK2 staining categories I and II. In contrast, among patients exhibiting nucleolar CK2 staining categories IV or V, 3 of 5 patients had been classified at p Stage I or IIA at first surgery, and later died of breast cancer. Kaplan-Meier analysis uncovered the association of nucleolar CK2α with poor prognosis among TN and late-stage breast cancers, which seemed significant. Hazard ratios further demonstrated that nucleolar CK2 staining offered another prognostic factor, in addition to lymph node metastatic status (Table 3). These findings, including multivariate hazard

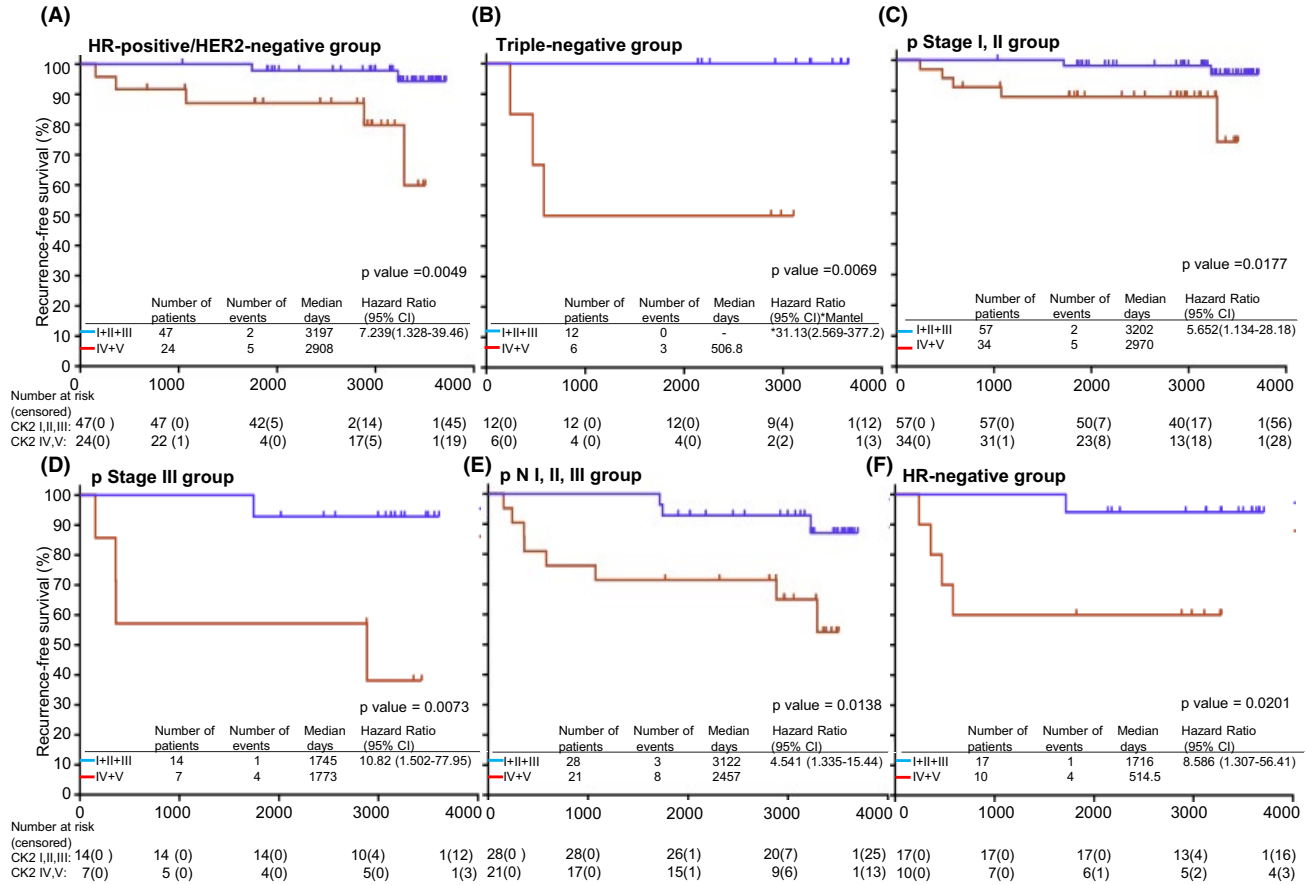

FIGURE 4 Positive nucleolar CK2α staining predicts poor prognosis among TN and late-stage cancers. RFS percentage is shown, stratified by combined CK2 staining categories in patients grouped according to hormone receptor (ER and/or PR)-positive/HER2-negative status (A, N = 71), TN status (B, N = 18), and pathological stage (p Stage) I or II (C, N = 91), p Stage III (D, N = 21), p N I to III (E, N = 49), or hormone receptor (ER and PR)-negative (F, N = 27), using the Kaplan-Meier method. Differences between subgroup curves were assessed using the log-rank test. CI, confidence interval; HR, hazard ratio

analysis, suggested that nucleolar CK2 staining could be used to predict which patients would need further treatment. As shown in the Partition platform (Figure S3), CK2 staining evaluation followed the Ki-67-positive index, suggesting a possible integration of multiple markers for predicting the length of RFS more precisely. Although mutant TP53 signatures have proven to be a strong prognostic factor in early-stage breast cancer,[17] evaluating nucleolar CK2 staining in combination with other indicators may allow a more accurate prediction of future recurrence or metastasis, which cannot be accomplished by current methods.

What are the functional consequences of abnormal CK2 behavior in breast carcinoma? CK2 complexes presented here in MCF-7 cells, a model breast cancer cell line, revealed a functional link of CK2 predominantly with protein synthesis, in which the role for CK2 in translation initiation was suggested by upregulated formation of eIF4F complexes through the mTORC1 pathway[18] and by CK2 phosphorylation of eIF5, a key molecule for translation initiation in vivo.[19] In addition, considering that high levels of rRNA synthesis by Pol I and ribosomal protein translation are important characteristics of highly proliferating cells, including cancerous cells, several recent studies of CK2 involvement in these systems have caught our attention. For example, CK2 is recruited to the rRNA gene promoter and directly regulates Pol I transcription by stabilizing the association of UBF with SL1.[20] A nucleolar transcription factor, UBF, which binds to 2 regions of the ribosomal DNA promoter is phosphorylated by CK2, eventually elevating transcription of ribosomal RNA.[21] Notably, a study of nucleolar proteomics in HeLa cells identified CK2 among 489 nucleolar proteins.[22] These results suggested that CK2 may help regulate to post-transcriptional modification of ribosomal RNAs and their stepwise maturation, by assembly with ribosomal proteins in the nucleolar and nuclear compartments. Studies are in progress to identify molecules in the CK2 complexes and/or downstream direct targets for CK2 phosphorylation that constitute a functional link between CK2 and malignant growth of breast cancers.

An important next step will be to determine the molecular mechanisms underlying CK2 accumulation, first in nuclei, and subsequently in nucleoli (Figure 1). One such mechanism may be the presence of a nucleolar translocation signal between positions 65 and 87 in CK2α, according to the Nucleolar Localization Sequence Detector.[23] We demonstrated the involvement of phosphorylation at multiple sites in CK2α, at Ser 7 and Ser 197, in relation to its activation and nuclear translocation in vivo (Homma MK et al, unpublished results). However,

TABLE 3 Nucleolar CK2α status as a precise, new prognostic factor

	Kaplan-Meier/Univariate			
Factor	**Chi-square**	**HR**	**95% CI**	**Log-rank, *P***
CK2 Nucleolar (+)	10.905	6.629	1.954-22.49	.0013
Tumor size, >2.0 cm	5.836	4.361	1.379-13.79	.0157
p Stage III	4.961	5.469	1.226-24.39	.0259
Nodal lymph, positive	11.349	14.3	4.568-44.78	.0008
Hormone receptor (−)	2.388	2.402	0.6251-9.23	.1222
Triple negative	0.9409	1.888	0.3872-9.209	.332
Histological grade 3	0.7998	1.678	0.4874-5.778	.3712
Ki67, ≥20%	1.957	2.188	0.6463-7.406	.1619
	Cox proportional hazards regression/univariate			
Factor	**Wald**	**HR**	**95%-CI**	***P*-value**
CK2 Nucleolar (+)	8.2	6.853	1.836-25.587	.004
Tumor size, >2.0 cm	4.887	4.37	1.182-16.153	.027
p Stage III	4.384	3.41	1.082-10.75	.036
Nodal lymph, positive	6.493	14.322	1.849-110.952	.011
Hormone receptor (−)	2.241	2.404	0.763-7.577	.134
Triple negative	0.91	1.889	0.511-6.983	.34
Histological grade 3	0.782	1.679	0.533-5.292	.367
Ki-67, ≥ 20%	1.860	2.211	0.707-6.912	.1726
	Cox proportional hazards regression/multivariate			
Factor	**Wald**	**HR**	**95%-CI**	***P*-value**
CK2 Nucleolar (+)	5.711	5.264	1.348-20.553	.017
Tumor size, >2.0 cm	3.616	1.837	0.414-8.152	.424
p Stage III	0.639	1.356	0.363-5.069	.651
Nodal lymph, positive	0.205	8.191	0.938-71.56	.057

Hazard ratio, confidence interval and *P*-values are compared between multiple diagnostic factors and nucleolar CK2α staining. Results from Kaplan-Meier and Cox proportional hazard regression analysis are shown.

Abbreviations: CI, confidence interval; HR, hazard ratio.

the molecular mechanism by which nucleolar CK2 promotes breast cancer recurrence is still obscure. Regulation of CK2 activity in nuclei and nucleoli also needs to be understood. Determining the functional consequences of nucleolar CK2 should facilitate the development of a treatment for IDC of the breast. This strategy was effective with CX-4945 against T-cell acute lymphoblastic leukemia cell lines, and a subcutaneous xenotransplant model of human T-ALL, demonstrating cytotoxic activity by downregulating PI3K/mTOR signaling,[24] and also against cultured breast cancer cells by downregulating the STAT3 axis and proliferation.[25] Therefore, CK2 inhibition could be relevant for breast cancer patients with nucleolar CK2α localization.

To confirm the specificity of CK2-positive staining in our study, histochemical staining experiments were performed repeatedly, sometimes compared with polyclonal antibodies against CK2α. The results demonstrated a unique specificity toward CK2α, as shown in Figure S4, in which similar results were obtained using serial sections from multiple formalin fixed paraffin-embedded blocks.

In summary, nucleolar CK2α localization is a useful marker for predicting adverse outcomes of patients with invasive ductal breast carcinomas who had undergone surgical resection of the tumor. This hypothesis provides a rationale for therapies with a CK2 inhibitor to tackle invasive malignancies, which may be associated with nucleolar dysfunction. Global clinical trials of CX-4945, a low-molecular-weight inhibitor of CK2α, are currently in progress. It is anticipated that nucleolar CK2-positive patients receiving aggressive post-operative treatment combined with a CK2 inhibitor may survive longer than those receiving standard chemotherapy. In addition, these findings may assist the development of anti-tumor strategies for breast cancers. If the efficacy of CK2 inhibition is verified, many patients globally will benefit.

ACKNOWLEDGMENTS

Miwako Kato Homma acknowledges funding by AMED under Grant Number 20lm0203006j0004. The authors are grateful to Katsuhiko Midorikawa at Hoshi General Hospital, and Moe Muramatsu at

Fukushima Medical University for experimental support, and Toshiyuki Suzuki at Fukushima Medical University for proteomics support. We thank the Biostatistical Consulting Service at Clinical Research Center, Fukushima Medical University, and in particular Dr Noriko Tanaka, who helped with the interpretation of the results from statistical analyses in this study. The authors thank Dr Natalie G. Ahn at the University of Colorado at Boulder, who kindly provided valuable discussion and comments. We thank Dr Steven D. Aird (www.sda-technical-editor.org) for editing the manuscript.

CONFLICTS OF INTEREST

The authors declare that they have no conflicts of interests.

AUTHOR CONTRIBUTIONS

MKH and TN designed and conceived the research. MKH and SM performed the experiments. YH, MN, NK, YH, and TN contributed analytic tools. MKH, YK, YH, SM, YH, and TN analyzed data. MKH, SM, and TN contributed data interpretation. MKH, and TN wrote the manuscript with input from all authors.

ORCID

Miwako Kato Homma https://orcid.org/0000-0002-5920-3596

REFERENCES

1. *WHO classification of tumors, Breast cancer*, (Rakha EA, Allison KH, Ellis IO, et al, Eds). 5th edn. 2019:82-101.
2. Forman D, Bray F, Brewster DH. *CI5PLUS: Cancer Incidence in Five Continents Vol. X IARC Scientific Publications No.164*, 1–1365. 164. 10th edn. Lyon: International Agency for research on Cancer, WHO; 2013. http://ci5.iarc.fr. https://ci5.iarc.fr/CI5I-X/old/vol10/CI5vol10.pdf.
3. Sobin LH, Gospodarowicz MK, Wittekind C. *TNM Classification of Malignant Tumours*, 7th edn USA: Wiley-Blackwell; 2011. ISBN:978-1-444-35896-4
4. Laible M, Hartmann K, Gürtler C, et al. Impact of molecular subtypes on the prediction of distant recurrence in estrogen receptor (ER) positive, human epidermal growth factor receptor 2 (HER2) negative breast cancer upon five years of endocrine therapy. *BMC Cancer*. 2019;19:694-702.
5. Sparano JA, Gray RJ, Makower DF, et al. Prospective validation of a 21-gene expression assay in breast cancer. *N Engl J Med*. 2015;373:2005-2014.
6. Bustreo S, Osella-Abate S, Cassoni P, et al. Optimal Ki-67 cut-off for luminal breast cancer prognostic evaluation: a large case series study with a long-term follow-up. *Breast Cancer Res Treat*. 2016;157:363-371.
7. Seldin DC, Leder P. Casein kinase II alpha transgene-induced murine lymphoma: Relation to theileriosis in cattle. *Science*. 1995;267:894-897.
8. Fleuren EDG, Zhang L, Wu J, Daly R. The kinome at large in cancer. *Nature Rev Cancer*. 2016;16:83-95.
9. Chua MM, Lee M, Dominguez I. Cancer-type dependent expression of CK2 transcripts. *PLoS One*. 2017;12(12):e0188854.
10. Yang L, Shi P, Zhao G, et al. Targeting cancer stem cell pathways for cancer therapy. Signal Transduction and Targeted. *Therapy*. 2019;5:8-35.
11. Gapany M, Faust RA, Tawfic S, Davis A, Adams GL, Ahmed K. Association of elevated protein kinase CK2 activity with aggressive behavior of squamous cell carcinoma of head and neck. *Mol Med*. 1995;1:659-666.
12. Landesman-Bollag E, Romieu-Mourez R, Song DH, Sonenshein GE, Cardiff RD, Seldin DC. Protein kinase CK2 in mammary gland tumorigenesis. *Oncogene*. 2001;20:3247-3257.
13. Rabalski AJ, Gyenis L, Litchfield DW. Molecular pathways: Emergence of protein kinase CK2(CSNK2) as a potential target to inhibit survival and DNA damage response and repair pathways in cancer cells. *Clinical Cancer Res*. 2016;22:2840-2847.
14. Homma MK, Shibata T, Suzuki T, et al. Role for protein kinase CK2 on cell proliferation: Assessing the components of the CK2 complex in the nucleus during the cell cycle progression. Protein Kinase CK2 Cellular Function in Normal and Disease States. *Adv Biochem Health Dis*. 2015;12:197-226.
15. Muramatsu M, Hayashi Y, Onishi T, Sakai M, Takai K, Kashiyama T. Rapid isolation of nucleoli from detergent purified nuclei of various tumor and tissue culture cells. *Exp Cell Res*. 1974;88:345-351.
16. Amano M. Metabolism of RNA in the liver cells of the rat. *Exp Cell Res*. 1967;46:169-179.
17. Yamaguchi S, Takahashi S, Mogushi K, et al. Molecular and clinical features of the TP53 signature gene expression profile in early-stage breast cancer. *Oncotarget*. 2019;9:14193-14206.
18. Gandin V, Masvidal L, Cargnello M, et al. mTORC1 and CK2 coordinate ternary and eIF4F complex assembly. *Nature Commun*. 2016;7:11127. https://doi.org/10.1048/ncomms.11127
19. Homma MK, Wada I, Suzuki T, Yamaki J, Krebs EG, Homma Y. CK2 phosphorylation of eukaryotic translation initiation factor 5 potentiates cell cycle progression. *Proc Natl Acad Sci USA*. 2005;102:15688-15693.
20. Panova T, Panov K, Russell JR, Zomerdijk JCBM. Casein kinase 2 associates with initiation-competent RNA polymerase I and has multiple roles in ribosomal DNA transcription. *Mol Cell Biol*. 2006;26:5957-5968.
21. Bienhoff H, Dundr M, Michels A, Grummt I. Phosphorylation by CK2 facilitates rDNA gene transcription by promoting dissociation of TIF-IA from elongating RNA polymerase I. *Mol Cell Bio*. 2008;28:4988-4998.
22. Andersen JS, Lam YW, Leung AKL, et al. Nucleolar proteome dynamics. *Nature*. 2005;433:77-83.
23. Scott MS, Boisvert FM, McDowall MD, Lamond AI, Barton GJ. Characterization and prediction of protein nucleolar localization sequences. *Nucleic Acids Res*. 2010;38:7388-7399.
24. Buontempo F, Orshin E, Martlins LR, et al. Cytotoxic activity of casein kinase 2 inhibitor CX-4945 against T-cell acute lymphoblastic leukemia: targeting the unfolded protein response signaling. *Leukemia*. 2014;28:543-553.
25. Gray GK, McFarland BC, Rowse AL, Gibson SA, Benveniste EN. Therapeutic CK2 inhibition attenuates diverse prosurvival signaling cascades and decreases cell viability in human breast cancer cells. *Oncotarget*. 2014;5:6484-6496.

SUPPORTING INFORMATION

Additional supporting information may be found online in the Supporting Information section.

How to cite this article: Homma MK, Kiko Y, Hashimoto Y, et al. Intracellular localization of CK2α as a prognostic factor in invasive breast carcinomas. *Cancer Sci*. 2021;112:619–628. https://doi.org/10.1111/cas.14728

SUPPORTING INFORMATION

Table S1: Protein lists in nuclear CK2 complexes from MCF-7 cells.

Table S2: Characterization of recurrent cases, stratified by breast carcinoma subtypes.

Supplemental Figure S1: Proteomic identification of nuclear CK2 interactors demonstrates functional involvement in the pathway leading to protein synthesis.

Supplemental Figure S2: Nucleolar CK2α status can predict future cancer recurrence in early stage patients.

Supplemental Figure S3: Nucleolar CK2 evaluation as a primary tool for predicting possible clinical outcomes.

Supplemental Figure S4: Comparing immunohistochemical detection of protein kinase CK2α using two different antibodies.

Table S1: **Protein lists in nuclear CK2 complexes from MCF-7 cells.**

Protein name	Accession	Quantitative	p-value
Histone H1.2	H12	5.91E+08	0.00033
Histone H1.5	H15	3.98E+08	0.002
Histone H4	H4	3.76E+08	0.017
Histone H3.3	H33	1.92E+08	0.0066
Epiplakin	EPIPL	8.61E+07	< 0.00010
Tubulin alpha-1C chain	TBA1C	8.40E+07	0.00054
Plectin	PLEC	7.63E+07	< 0.00010
Heterogeneous nuclear ribonucleoproteins C1/C2	B2R5W2	5.47E+07	0.0025
Heat shock cognate 71 kDa protein	HSP7C	5.36E+07	< 0.00010
Tubulin beta chain	TBB5	4.97E+07	< 0.00010
Actin, cytoplasmic 2	ACTG	4.94E+07	< 0.00010
Heat shock 70 kDa protein 1B	A0A0G2JIW1	4.71E+07	< 0.00010
RNA-binding protein 14	RBM14	4.05E+07	< 0.00010
Putative elongation factor 1-alpha-like 3	EF1A3	3.52E+07	< 0.00010
ADP/ATP translocase 2	ADT2	3.25E+07	< 0.00010
Prelamin-A/C	LMNA	2.60E+07	< 0.00010
Stress-70 protein, mitochondrial	GRP75	2.33E+07	0.00022
Heterogeneous nuclear ribonucleoproteins A2/B1	ROA	2.27E+07	< 0.00010
Cytochrome c oxidase subunit 5B, mitochondrial	COX5B	2.10E+07	0.0059
Desmoplakin	DESP	1.81E+07	< 0.00010
Heterogeneous nuclear ribonucleoprotein M	HNRPM	1.72E+07	< 0.00010
Filamin-A	Q5HY54	1.70E+07	0.00082
Lamin-B1	LMNB1	1.68E+07	0.0013
Heterogeneous nuclear ribonucleoprotein F	HNRPF	1.67E+07	< 0.00010
RNA-binding motif protein, X chromosome	RBMX	1.67E+07	< 0.00010
ATP synthase subunit alpha, mitochondrial	ATPA	1.41E+07	< 0.00010
60S ribosomal protein L6	Q9HBB3	1.19E+07	0.0074
ATP synthase subunit beta, mitochondrial	ATPB	1.16E+07	< 0.00010
Prohibitin-2	F5GY37	1.07E+07	< 0.00010
Prohibitin (Fragment)	C9JW96	1.03E+07	< 0.00010
Splicing factor proline/glutamine-rich	Q86VG2	8693800	0.025
Heterogeneous nuclear ribonucleoprotein A1	F8W6I7	7785600	0.00075

MICOS complex subunit MIC60	B4DKR1	4912100	0.00012
Filamin B, beta	A0A024R321	4846900	0.00029
Elongation factor Tu, mitochondrial	EFTU	1689700	< 0.00010

Protein name, accession number, quantitative values after normalization and ANOVA test, and p-value are shown. Peptide threshold, all 95.0% with minimum two peptides.

Table S2: Characterization of recurrent cases, stratified by breast carcinoma subtypes.

Subtype	CK2α	ID	Age	p Stage	Tumor size (cm)	pT	pN	Histological grade	Nodal lymph (number)	RFS (days)	Died
Triple negative	V	#40	55	I	2	1c	0	3	0	471	●
	V	#83	68	IIA	2	1c	1	3	3	582	●
	IV	#75	72	IIA	2	1c	1	2	3	242	●
Hormone receptor (-), HER2 (+)	IV	#92	37	ⅢC	11	4	3	3	23	358	
	III	#16	56	IIB	3.2	2	1	2	1	1716	
Hormone receptor (+), HER2 (-)	V	#03	46	ⅢC	5	2	3	3	17	2884	
	V	#56	42	IIB	2.5	2	1	2	1	1075	
	IV	#06	69	ⅢC	2.5	2	3	2	20	156	●
	IV	#19	53	ⅢC	12	4a	3	1	18	361	
	IV	#51	44	IIB	2.2	2	1	2	1	3292	
	III	#13	38	IIB	3.5	2	1	3	2	3229	
	III	#70	35	ⅢA	3.5	2	2	1	7	1745	●

Recurrent cases in this study are summarized by age, p Stage, tumor size, pT, pN, histological grade, lymph node status, and days of recurrence free survival. A death after a recurrence is marked with a black dot circle.

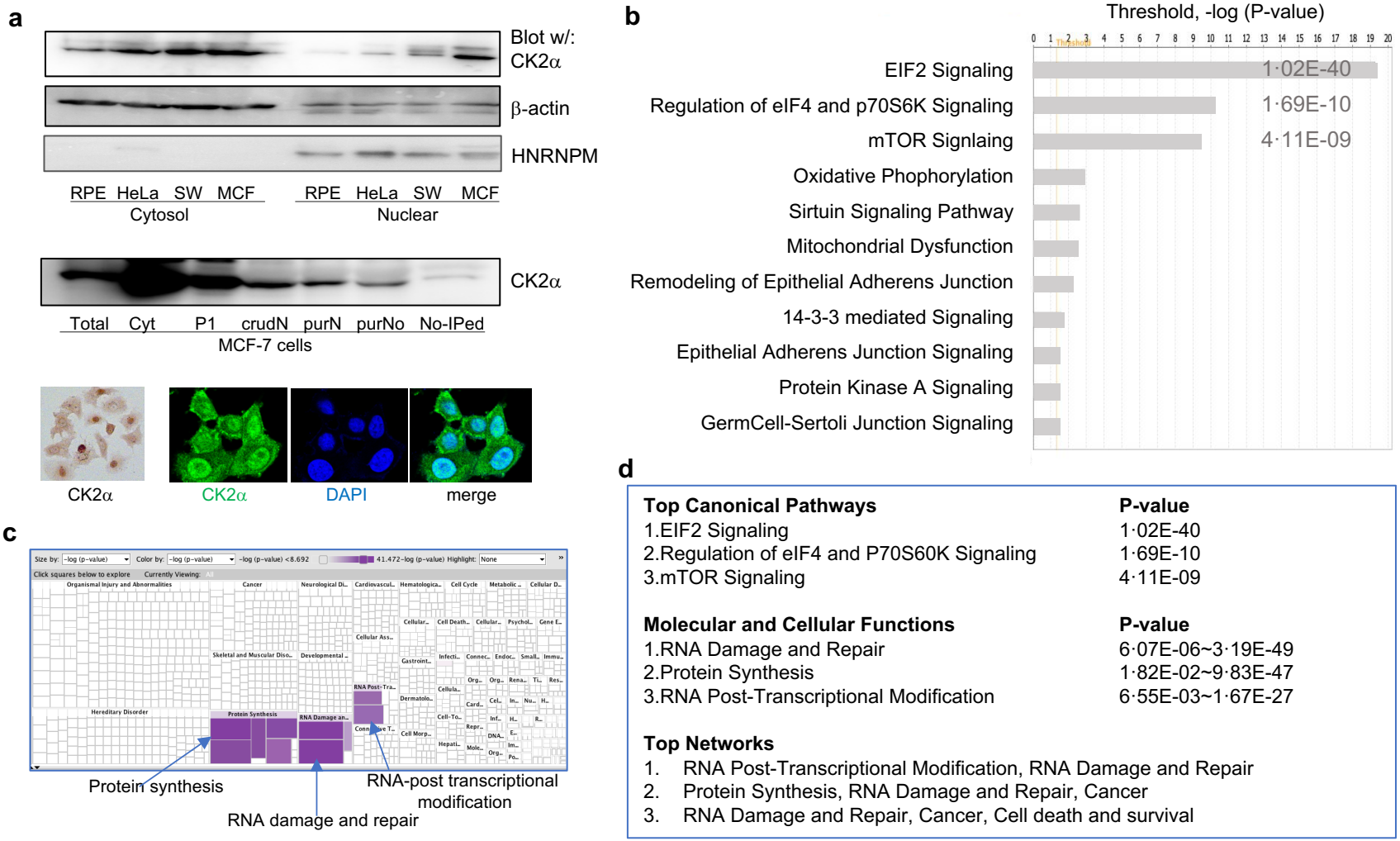

Top Canonical Pathways	P-value
1.EIF2 Signaling	1·02E-40
2.Regulation of eIF4 and P70S60K Signaling	1·69E-10
3.mTOR Signaling	4·11E-09

Molecular and Cellular Functions	P-value
1.RNA Damage and Repair	6·07E-06~3·19E-49
2.Protein Synthesis	1·82E-02~9·83E-47
3.RNA Post-Transcriptional Modification	6·55E-03~1·67E-27

Top Networks

1. RNA Post-Transcriptional Modification, RNA Damage and Repair
2. Protein Synthesis, RNA Damage and Repair, Cancer
3. RNA Damage and Repair, Cancer, Cell death and survival

Supplemental Figure S1: **Proteomic identification of nuclear CK2 interactors demonstrates functional involvement in the pathway leading to protein synthesis. a,** (*Upper*) Western blot showing subcellular localization of CK2α protein at much higher levels in cancer cells. RPE was derived from normal retina pigment epithelium. HeLa was derived from cervical cancer cells. SW-480 is a colorectal carcinoma with active *ras* and truncated *APC* mutations, and MCF-7 is a breast carcinoma. (*Middle*) Cell fractionation of MCF-7 cells according to references, [15,16] stages of which are as follows: total lysate, cytosolic, first precipitates, crude or more purified nuclear extract, purified nucleolar extract, and anti-CK2α immunoprecipitates of the nucleolar extract. (*Lower*) Cell images of MCF-7 cells employing anti-CK2α antibodies, visualized with DAB staining (left) or Alexa Fluor 488-conjugated secondary antibody, accompanied by images using DAPI. **b-d**, CK2-immunoprecipitated nuclear proteins from MCF-7 cells and RPE cells were identified using nanoflow LC-MS analysis. Lists of proteins in the CK2 complexes with higher expression and unique to MCF-7 cells, compared to those in RPE cells, with ANOVA test p-value below 0.05, are shown in Supporting Information Table S1, and further analyzed by IPA in order to demonstrate top canonical pathways (**b**), and top functions (**c**). Predicted molecular and cellular functions are shown in **d**. *P*-values are indicated when the difference was statistically significant.

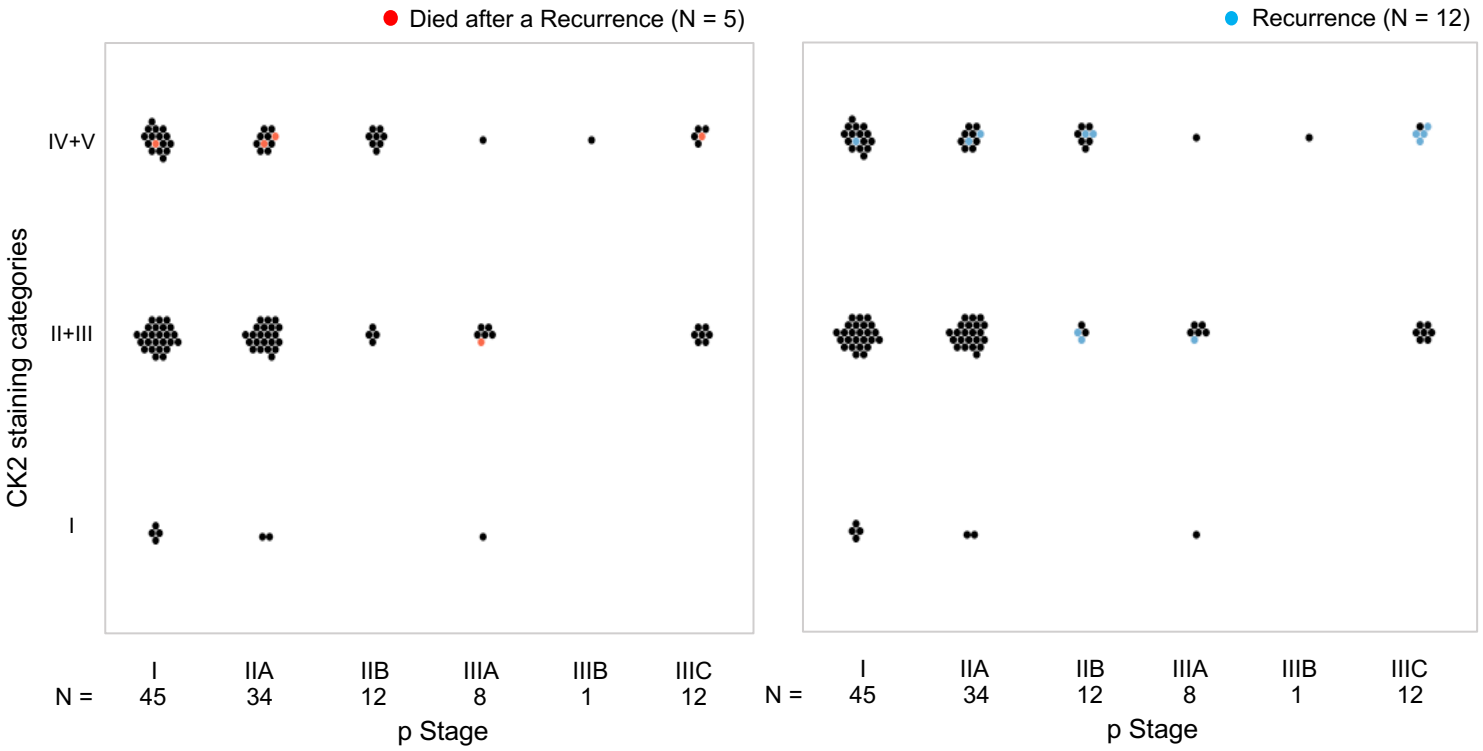

Supplemental Figure S2: **Nucleolar CK2α status can predict future cancer recurrence in early stage patients.**
Each black dot represents one patient, diagnosed according to p Stage (X-axis) and CK2 staining status (Y-axis). n=112 cases. Patients who died after a recurrence (left, N=5) or who recurred (right, N=12) are shown with red or blue dots, respectively.

a

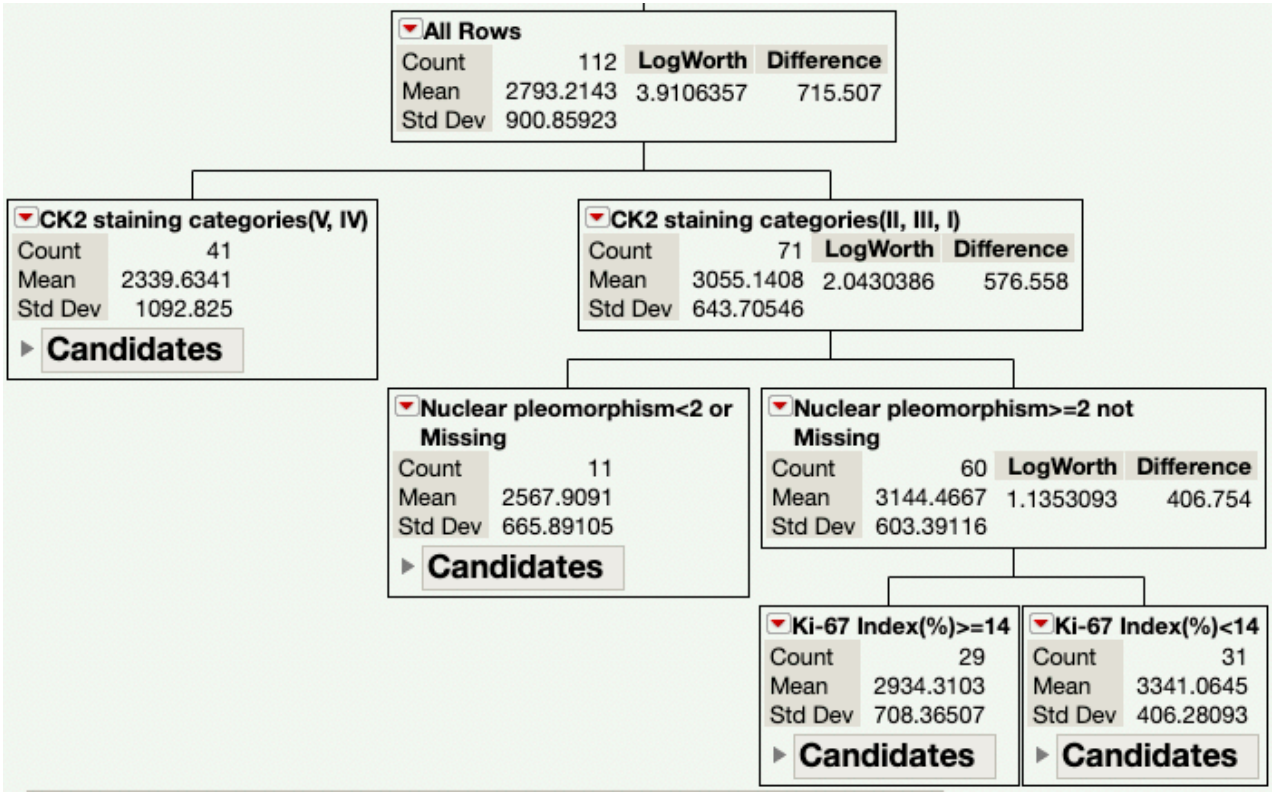

b

Column Contributions

Term	Number of Splits	SS	Portion
CK2 staining categories	1	13306124.8	0.7050
Ki-67 index(%)	1	3090088.75	0.1637
Nuclear pleomorphism	1	2478976.86	0.1313
Tumor size	0	0	0.0000
pStage	0	0	0.0000
Subtype	0	0	0.0000
Tubular formation	0	0	0.0000
Histological grade	0	0	0.0000
Nodal metastatic status	0	0	0.0000
Age	0	0	0.0000

Supplemental Figure S3: Nucleolar CK2 evaluation as a primary tool for predicting possible clinical outcomes.
a, A decision tree created by multiple factors to predict the length of patient RFS, showing nucleolar CK2-positive (IV, V) or -negative (I, II, III) evaluation at the first level (row), and the latter categories are followed by nuclear pleomorphism and Ki-67 index.
b, Clinicopathological information attributed to the cluster analysis is shown. Column contribution delineates CK2 staining evaluation contributes the most to predicting the variation in future length of survival.

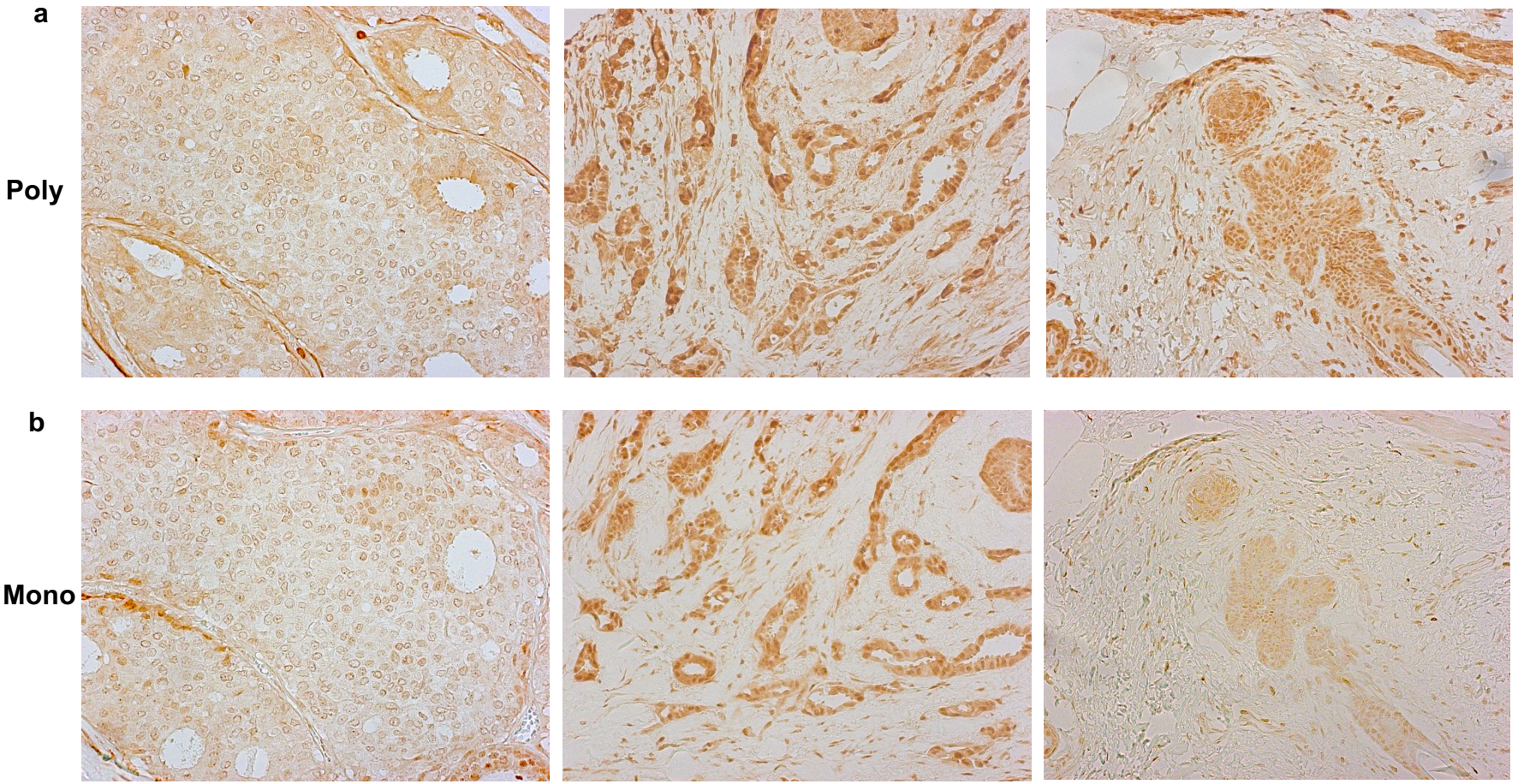

Supplemental Figure S4: Comparing immunohistochemical detection of protein kinase CK2α using different antibodies. Serial sections of FFPE blocks from IDC breast cancer are stained with either of two antibodies raised against CK2**α**, from rabbit polyclonal antibodies (**a***), or mouse monoclonal antibody, which is used in this study (**b**). Both stain CK2α in the nucleus as well as in the nucleolus. Higher false-positive staining was observed when using polyclonal antibodies.

*Ref: Litchfield DW, Lozeman F, Piening CP, Sommercorn J, Takio K, Walsh KA, Krebs EG. Subunit structure of casein kinase II from bovine testis. Demonstration that the α and α' are distinct polypeptides. *J Biol Chem* 1990; 265: 7638-7644.